

Modal control in semiconductor optical waveguides with uniaxially patterned layers

Arsen V. Subashiev, and Serge Luryi, *Fellow, IEEE*

Abstract—Uniaxially patterned dielectric layers have an optical anisotropy that can be externally controlled. We study the effects of patterning the cladding or the core layer of a 3-layer optical waveguide on the polarization properties of propagating radiation. Particular attention is paid to the case when the core material is a semiconductor with optical gain. We discuss a number of devices based on incorporating an uniaxially patterned layer in the structure design, such as a polarization-insensitive amplifier, a polarizer, an optically-controlled polarization switch, and an optically controlled modal coupler.

Index Terms—Semiconductor lasers, dielectric waveguides, photonic crystals, optical polarizers, directional couplers

I. INTRODUCTION

STRUCTURES with cylindrical air pores forming a 2-d periodic lattice in a semiconductor material are actively studied for photonic bandgap applications, [1], [2], [3] such as spontaneous emission control and light confinement in micro-cavities. These studies stimulated numerous computations of the photonic crystal (PC) band spectra, based on the plane wave expansion of the electromagnetic field [4], [5]. Such calculations showed that in the long wavelength limit the spectrum of electromagnetic waves can be well described in the effective media approximation with an effective dielectric constant corresponding to the results of Maxwell Garnett theory [6], [7], [8]. Optical properties of the composite structures patterned with cylindrical holes, for the wavelength exceeding the interhole spacing a , i.e., for $\lambda \gg a$, are described in terms of the filling factor f alone (i.e. the fraction of the total volume occupied by the pores), and do not depend on the long-range order of the holes or their diameter. The effect of disorder is only a weak Rayleigh-like scattering. The effective media approach remains valid for very large contrast ratios between the semiconductor and the pore permittivities [9], [10], [11] and for arbitrary propagation directions of the electromagnetic waves. Direct comparison of the calculation results based on 3-d and 2-d modeling shows that the same approach can be used to describe the waveguiding properties of multi-layered structures that include patterned layers. Moreover, studies of PC-like structures with

a small disorder showed that the Maxwell Garnett approach remains valid even when the requirement $\lambda \gg a$ is relaxed to $\lambda > a$, so long as the optical frequency is below the photonic bandgap and light scattering remains negligible (similar situation prevails in electronic spectra engineering with quantum well and superlattice heterostructures).

In this paper we explore variable anisotropic optical properties of uniaxially patterned (UAP) layers and find that they can be useful in the design of numerous optical devices that are sensitive to the shape and polarization of the optical mode, such as polarizers, lasers, amplifiers and modulators. The UAP anisotropy is not accompanied by any additional optical loss and therefore can be used effectively for the modal control of optical emitters and amplifiers.

Polarization sensitivity is an important factor in semiconductor lasers and amplifiers. It depends on the modal gain which in turn depends on both the material gain anisotropy and the mode confinement factor [12]. The traditional 3-layer waveguide design of semiconductor amplifiers with isotropic constituents leads to a better confinement of the TE mode and a larger modal gain for this mode compared to the TM mode [13], [14]. To obtain a polarization-insensitive amplifier one had to use highly anisotropic active layers with the material gain that favors TM polarization. Adoption of UAP media for the waveguide layers, gives an additional possibility to compensate for the difference in the TE-TM confinement, inherent to the isotropic situation.

Possible applications of the waveguide structures with a UAP layer extend to the territory already tested experimentally for PC layers, such as structures with a periodically patterned cladding layer, e.g. [2] and periodically patterned active layer, e.g. [15], [16]. For the UAP structures we consider, the pattern long-range order is of no consequence. The relative value of modal propagation constants can be altered by varying the thickness of the core region or by varying the fill-factor of the patterned layer. The propagation constants can be further fine-tuned by changing the optical contrast between the waveguide constituents with an applied field or optical pumping. Tuning effects are enhanced in structures that are particularly sensitive to the anisotropy of each layer, such as asymmetric waveguides with a thin core layer.

II. DIELECTRIC FUNCTION OF UNIAXIALLY PATTERNED LAYERS AND THE WAVEGUIDE MODES

Anticipating a broad scope of possible applications we consider a 3-layer waveguide in which all three layers, the top cladding (c), the core (f), and the substrate or bottom

Based on manuscript submitted May 3, 2005 to IEEE J. of Lightwave Technology. This work was supported by the NY State Center for Advanced Sensor Technology (Sensor CAT) at Stony Brook.

Arsen V. Subashiev is with the Department of Electrical and Computer Engineering, State University of New York at Stony Brook, Stony Brook, NY, 11794-2350, on leave from the State Polytechnic University, St. Petersburg, Russia, 195251 (e-mail:subashiev@ece.sunysb.edu).

Serge Luryi is with the Department of Electrical and Computer Engineering, State University of New York at Stony Brook, Stony Brook, NY, 11794-2350 (e-mail:Serge.Luryi@stonybrook.edu).

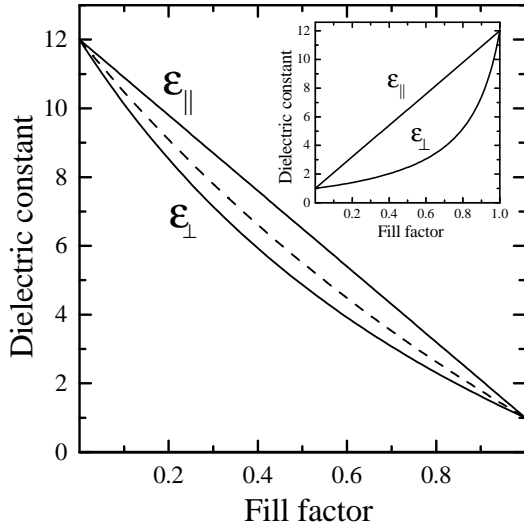


Fig. 1. Average permittivities $\epsilon_{||}$ and ϵ_{\perp} of a silicon ($\epsilon_{out} = 12$) layer uniaxially patterned with cylindrical air pores ($\epsilon_{in} = 1$) for $E \parallel C$ and $E \perp C$, respectively. The dotted line shows the average refractive index (squared). The inset shows the $\epsilon_{||}$ and ϵ_{\perp} for a mirror structure of dielectric cylinders, ($\epsilon_{in} = 12$, $\epsilon_{out} = 1$).

cladding (s), may be uniaxially patterned. We assume a thin core layer (of thickness d) that can support only the lowest propagation modes. We examine the case when the optical axis C of the patterned layers is perpendicular to the waveguide plane. We denote by $\epsilon_{k||f;s}$ and $\epsilon_{?||f;s}$ the permittivities of the ϵ_s , ϵ_f , or ϵ_s layers for two directions of the electric field, parallel (k) and perpendicular ($?$) to the optical axis, respectively. The permittivity of the inhomogeneous medium in a long-wavelength limit is obtained in the Maxwell Garnett approximation.

For s-polarization ($E \perp C$), the permittivity of a 2-d array of infinitely long cylinders is obtained by direct averaging, viz.

$$\epsilon_{\perp} = \epsilon_{out} + (\epsilon_{in} - \epsilon_{out})f; \quad (1)$$

where the permittivity ϵ_{in} is inside and ϵ_{out} outside the cylinder.

For p-polarization ($E \parallel C$) the permittivity is given by

$$\epsilon_{||} = \epsilon_{out} \frac{(\epsilon_{in} + \epsilon_{out}) + (\epsilon_{in} - \epsilon_{out})f}{(\epsilon_{in} + \epsilon_{out}) - (\epsilon_{in} - \epsilon_{out})f}; \quad (2)$$

The dependence of $\epsilon_{||}$ and ϵ_{\perp} on the filling factor is shown in Fig. 1 for the case of cylinder pores in a dielectric medium, with $\epsilon_{in} = 1$ and $\epsilon_{out} = 12$. The anisotropy of refractive index is evidently not small, e.g., for $f = 0.3$, one has $(n_k - n_?) = \sqrt{\epsilon_{||} - \epsilon_{\perp}} = 0.1$. Also shown is the value of permittivity that would correspond to an average refractive index, i.e. $\langle n \rangle = n_{in}f + n_{out}(1 - f)$ which is sometimes used, see e.g. [17], without a reasonable justification [18].

The inset to Fig. 1 shows the permittivities $\epsilon_{||}$ and ϵ_{\perp} for a "mirror" array of cylindrical rods in air. This geometry offers a substantially higher optical anisotropy. Mathematically, it is described by Eqs. (1) and (2) with the replacement $\epsilon_{out} \rightarrow \epsilon_{in}$.

Note that Eq. (2) fails for thin UAP layers, when the height of the cylinders becomes comparable to their diameter. For

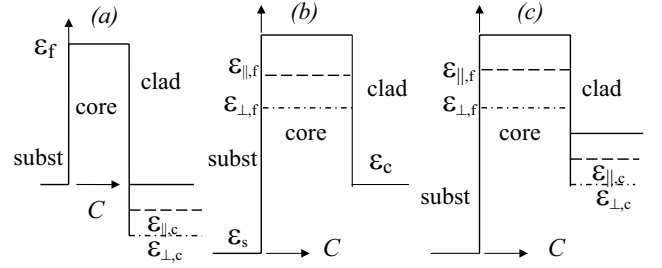


Fig. 2. Profile of the dielectric function in the 3-layers waveguide with PL layers: patterned cladding layer (a), patterned core layer (b) and patterned core and cladding layers (c).

this case the effective media approach remains valid, but Eq. (2) must be modified to allow for depolarization factors of the finite-height cylinders.

Below, we discuss properties of a 3-layer waveguide. We shall employ the usual approach [12] developed for isotropic waveguide constituents. The guided modes supported by the structure will be calculated using the values n_k and $n_?$ as polarization-dependent refractive indices of the patterned layers. Exemplary profiles of the dielectric function are shown in Fig. 2 for a waveguide with patterned cladding layer (a), an asymmetric waveguide with a UAP core layer, (b), and a hypothetical structure with both cladding and core layers patterned (c).

A. TE mode

In the TE mode the electric field is perpendicular to the pore axes, so that *ordinary* waves propagate in all 3 layers. Therefore, in order to find the modal index, we can use the eigenvalue equation for the propagation wave vector in an isotropic layered structure [12]

$$k_{o,f}d = \tan^{-1}(\epsilon_{||f}/\epsilon_{||s}) + \tan^{-1}(\epsilon_{||s}/\epsilon_{||f}) \quad (3)$$

in which the substitution $\epsilon_{||f} \rightarrow \epsilon_{||f;s}$ should be made, viz., where $k_{o,f} = \sqrt{\epsilon_{||f} - Q^2}$, $\epsilon_{||f} = \epsilon_{||f;s}$, $\epsilon_{||s} = \sqrt{\epsilon_{||s} - Q^2}$, $k_0 = \sqrt{\epsilon_{||s} - Q^2}$, and Q is the propagation wave vector, which defines the mode effective index, $n_{eff} = Q/k_0$.

From Eq. (3) the cutoff thickness $d_{c,TE}$ of the active layer for the case $\epsilon_{||s} > \epsilon_{||f}$ is given by

$$d_{c,TE} = \frac{1}{k_0(\epsilon_{||f} - \epsilon_{||s})} \tan^{-1}\left(\frac{\epsilon_{||s}}{\epsilon_{||f}}\right); \quad (4)$$

where a_{TE} is an asymmetry parameter of the form

$$a_{TE} = \frac{\epsilon_{||s} - \epsilon_{||f}}{\epsilon_{||f} - \epsilon_{||s}} \quad (5)$$

The case $\epsilon_{||s} < \epsilon_{||f}$ is described by replacing $\epsilon_{||s} \rightarrow \epsilon_{||f}$.

In the limit of a very thin active layer, $k^2 d \ll 1$, equation (3) yields

$$n_{eff,TE} = \frac{\epsilon_{||f}}{\epsilon_{||s}} + \frac{2}{2\epsilon_{||f}}; \quad (6)$$

where

$$\epsilon_{||f} = \frac{k_0^2 d^2 (\epsilon_{||f} - \epsilon_{||s})^2}{2k_0 d (\epsilon_{||f} - \epsilon_{||s})} \quad (7)$$

For an amplifying structure with active core, the gain factor for the TE mode g_{TE} can be calculated as follows [13]:

$$g_{TE} = \frac{k_0}{n_{eff,TE}} \frac{\int_0^d dx \int_0^d dy \mathbf{E}_y \cdot \mathbf{J}_y}{\int_0^d dx \int_0^d dy \mathbf{E}_y \cdot \mathbf{J}_y}; \quad (8)$$

where ϵ_f^{im} is an imaginary part of the active layer permittivity, x is taken along C and y perpendicular to the wave propagation direction. For a UAP core, the integration in Eq. (8) includes taking the average over the layer plane. The modal gain (8) can be written as a product of the material gain $g_f = k_0 \frac{\epsilon_f^{\text{im}}}{\epsilon_f^{\text{re}}}$ and the optical confinement factor, Γ_{TE} , which can be calculated explicitly in the dipole approximation for the field distribution in the patterned layer. For a structure with a thin patterned core layer, Γ_{TE} equals

$$\Gamma_{TE} = s \frac{\frac{f_{out}}{s}}{\frac{f_{out}}{s} + \frac{2}{s} \frac{c + \frac{2}{\Gamma_{TE}}}{c + \frac{2}{\Gamma_{TE}} + \Gamma_{TE}}} \Gamma_{TE} k_0 d; \quad (9)$$

where s is the local field factor $s = (1 + B^2 f) = (1 + B f)^2$, and $B = (\epsilon_{f,out} - \epsilon_{f,in}) = (\epsilon_{f,out} + \epsilon_{f,in})$. For a symmetric waveguide, Eq. (9) reduces to the well-known result [20]. For an asymmetric waveguide, Γ_{TE} rapidly decreases with the difference of the indices of the cladding and substrate layers, as follows from Eq. (7). This leads to a high sensitivity of the optical confinement to both the asymmetry of the waveguide and the layer anisotropy.

B. TM mode

For the TM mode the electric field has two components, one perpendicular and the other parallel to the C axis. The propagating waves are *extraordinary* in the UAP layers. The eigenvalue equation is of the form

$$k_{ef} d = \tan^{-1} \frac{\epsilon_f^{\text{im}}}{\epsilon_{fc} k_{ef}} + \tan^{-1} \frac{\epsilon_f^{\text{im}}}{\epsilon_{fs} k_{ef}}; \quad (10)$$

where

$$k_{ef} = \frac{q}{\epsilon_f^{\text{re}} k_0^2} \left(\epsilon_f^{\text{re}} - k_{ef}^2 \right) Q^2;$$

$$c = \frac{q}{(\epsilon_f^{\text{re}} - k_{ef}^2) Q^2} \epsilon_{fc} k_0^2;$$

and

$$s = \frac{q}{(\epsilon_f^{\text{re}} - k_{ef}^2) Q^2} \epsilon_{fs} k_0^2;$$

The cutoff thickness $d_{c, TM}$, for a structure with $k_{fs} > k_{fc}$ is given by

$$d_{c, TM} = k_0 \frac{q}{(\epsilon_f^{\text{re}} - k_{ef}^2) (\epsilon_{fc} - k_{fs}^2)} \tan^{-1} \left(\frac{1}{a_{TM}} \right); \quad (11)$$

where the asymmetry parameter a_{TM} has the form

$$a_{TM} = \frac{\epsilon_f^{\text{re}} k_{ef} (\epsilon_{fs} - k_{fc}^2)}{\epsilon_{fc} k_{fc} (\epsilon_{fs} - k_{ef}^2)} \quad (12)$$

The case $k_{fs} < k_{fc}$ is described by replacing k_{fs} with k_{fc} and ϵ_{fs} with ϵ_{fc} .

For a very thin active layer, $k_{fx}^2 d \ll 1$, Eq. (10) yields

$$n_{eff, TM} = \frac{1}{k_{fs}} + \frac{2}{2} \frac{\Gamma_{TM}}{k_{fs}}; \quad (13)$$

where

$$\Gamma_{TM} = \frac{k_0^2 d^2 r_1^2 (\epsilon_{fs} - k_{ef}^2)^2}{2 k_0 d r_1 (\epsilon_{fs} - k_{ef}^2)}; \quad \Gamma_{TM} = 1 \quad (14)$$

with $r_1 = \frac{1}{k_{fs} - k_{ef}^2}$, and $r_2 = \frac{1}{k_{fs} - k_{fc}^2}$.

In calculations of the modal gain g_{TM} and the optical confinement Γ_{TM} for the TM mode one must correctly evaluate the energy flux in and outside the active layer [13]. We write down the optical confinement factor for a structure with a thin patterned core layer,

$$\Gamma_{TM} = (1 - f) \frac{s \frac{f_{out}}{s}}{\frac{f_{out}}{s} + \frac{2}{s} \frac{c + \frac{2}{\Gamma_{TM}}}{c + \frac{2}{\Gamma_{TM}} + \Gamma_{TM}}} \Gamma_{TM} k_0 d \quad (15)$$

As follows from Eqs. (14,15), due to a small multiplier r_1^2 in the numerator of (14), both Γ_{TM} and hence g_{TM} are even more sensitive to the asymmetry and anisotropy than the analogous parameters for the TE-mode. When the active layer is thin, $k_{fx}^2 d \ll 1$, the confinement for the TM mode is smaller by a factor of $(s - f)^3$ than that for the TE mode. For thicker layers, $k_{fx}^2 d \gg 1$, this ratio reduces to $(s - f)^2$, see e.g. [13], [14].

The mode competition in laser structures is also affected by the difference in the reflection coefficients for the competing modes. For a cleaved stripe structure the modal reflection coefficients R_m are given by [21]

$$R_m = \frac{(n_{eff, m} - 1)^2}{(n_{eff, m} + 1)^2}; \quad m = TE, TM; \quad (16)$$

Thus, in the effective index approach this ratio is a function of $n_{eff, TE}$ and $n_{eff, TM}$ and, therefore, is also affected by the fill factor of the UAP layers of the waveguide.

III. POSSIBLE APPLICATIONS OF UAP STRUCTURES

We have shown that the cutoff thicknesses and modal propagation constants in waveguides with a thin core layer are sensitive to the permittivities of the layers and their patterning. Small variations of the propagation constants result in substantial changes of the confinement factors modal ratio. This modal control can be employed in optical devices, such as polarizers and mode-insensitive amplifiers. It is important to realize that the control can be effected rapidly and in real time. For example, optical pumping of the UAP layer within the absorption band of one of its constituent materials will change the optical contrast of the uniaxial pattern and thus modify both the refractive index of the UAP layer and the modal indices of the waveguide. Thus, we can have an ultra-fast switch of the modal response in an anisotropy-based cut-off device. Other possible applications are mode-dependent leaky waveguides and directional couplers. With an additional high-index layer, adjacent to one of the cladding layers, the coupling of waveguide modes to this layer will have a strong dependence on the matching of modal propagation constants.

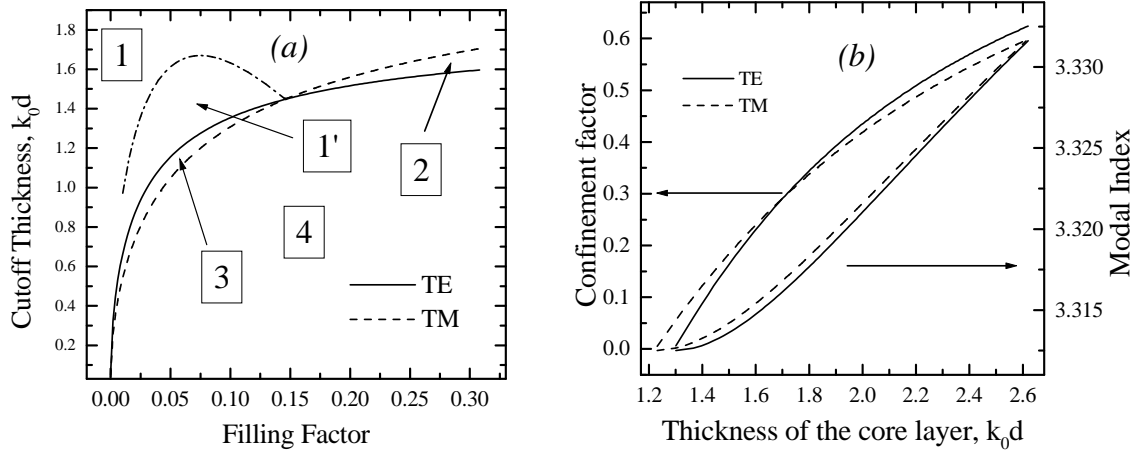


Fig. 3. (a) Cutoff thicknesses for TE and TM modes as functions of the fill-factor in the UAP cladding layer for $\text{Al}_{0.17}\text{Ga}_{0.83}\text{As}/\text{GaAs}/\text{Al}_{0.17}\text{Ga}_{0.83}\text{As}$ structure. Four distinct mode confinement regions are identified: (1) both modes are confined, (2) only TE mode is confined, (3) only TM mode is confined, and (4) both modes are not confined. The dash-dotted line corresponds to the locus of points on the graph, where the confinement of both modes is the same. It delineates a region (1') within (1) where $\gamma_{\text{TM}} > \gamma_{\text{TE}}$. (b) Variation of the optical confinement factors and the modal indices of the two modes with the active layer thickness d in a UAP structure as in (a) for a fixed filling factor $f=0.08$. Equal modal gain at $\lambda = 860$ nm is achieved for $d = 182$ nm.

A. Mode tuning and polarization-insensitive amplifier

To clarify the effects of a UAP layer on the waveguide modal properties, we consider the cutoff thickness of a symmetric 3-layer waveguide, in which one of the cladding layers is patterned, cf. the index profile of Fig. 1(a). Exemplary material compositions are taken for a GaAlAs heterostructure, specifically, GaAs core and $\text{Al}_x\text{Ga}_{1-x}$ with $x=0.17$ for both the cladding and the substrate layers. We assume the UAP structure in the cladding layer (cf. the structure of Ref. [2]). The alloy refractive index is taken in the form $n(x) = 3.4 - 0.53x + 0.09x^2$, [22].

Variation of the cutoff thicknesses $d_{c, \text{TE}}$ and $d_{c, \text{TM}}$ with the fill factor is shown in Fig. 3(a) in units of $1=k_0$. Both modes are confined in region 1, and neither mode is supported in region 4. Region 2 supports only the lowest TE mode and region 3 only the lowest TM mode. For a fill-factor $f = 0.141$ we see that $d_{c, \text{TE}} < d_{c, \text{TM}}$ and we can have a waveguide which supports only the lowest TM wave. For $\lambda = 0.86 \mu\text{m}$ and $f = 0.08$, the interval where this is the case is $167 \text{ nm} < d < 177 \text{ nm}$. Similarly, for $f = 0.141$ there is an interval of layer thicknesses in which only TE mode is confined. The reversal of modal confinement is due to a rapid decrease with f of the cladding layer indices for both polarizations. This leads to a better confinement of the TE mode at large f , since in a strongly asymmetric waveguide, the anisotropy is of minor importance.

The fact that $d_{c, \text{TE}} < d_{c, \text{TM}}$ in a certain range of fill-factors indicates that there is a *region* of core thicknesses in the *same range* where both modes are supported but the TM mode has a tighter optical confinement. This region, designated as 1', is delineated in Fig. 3(a) by the dash-dotted line. In the vicinity of the dash-dotted line there is another line where gain is mode-insensitive (precise position of this line depends on other factors, such as anisotropy of the material gain and modal dependence of the feedback). This enables us to design a mode-insensitive amplifier without relying on those other

factors.

It should be noted that in a waveguide with active (amplifying or absorbing) layers, the waveguiding itself is influenced by the gain/damping effects. For structures with a thin core layer, $k_0 d \ll 1$, these effects, however, are smaller than the index-guiding effects by a factor of $(k_0 d)^2$, see Appendix I, and they can be safely neglected.

Figure 3(b) shows the variation of optical confinement factors and effective modal indices as functions of the active layer thickness for an exemplary fill-factor $f = 0.08$. Equal confinement is obtained at $d = 1.62 \mu\text{m}$ ($k_0 d = 221.6$ nm (for $\lambda = 860$ nm)). Since at this thickness $n_{\text{eff, TE}} < n_{\text{eff, TM}}$, the design of a mode-insensitive amplifier should also take into account the different modal reflection coefficients, cf., e.g., (16).

Pore spacings ~ 100 nm and pore diameters ~ 30 nm [15], [16] are demanding but achievable with focused ion beam patterning. Parameters of the structure discussed above are adequately addressed with an approximately triangular lattice of pores of diameter 40 nm and pitch $a = 134$ nm. For such a lattice, the pitch remains comfortably shorter (~ 2 times) than the wavelength in the media. Requirements to the structure parameters are less demanding in the infrared region.

Equal modal confinement can also be obtained in the conceptually simpler (though probably less practical) case when the UAP layer is the core of a symmetric waveguide. This case can be easily analyzed in a similar fashion. We find that with a thin active layer the TM mode can be made competitive if one uses a waveguide with a relatively small initial index contrast, which makes it more sensitive to the core layer anisotropy. The desired low contrast is obtained by an appropriate choice of the fill-factor of the patterned core layer and the cladding layers composition.

B. Cutoff polarizer

In waveguides based on III-V heterostructures, the index contrast between the core and the cladding layers is weak. Because of this, the modal competition takes place at small f and for a thin core. The region of competition can be made substantially larger in asymmetric waveguides with properly chosen compositions in the substrate and cladding layers. For the $\text{Al}_x\text{Ga}_{1-x}\text{As}/\text{GaAs}/\text{Al}_y\text{Ga}_{1-y}\text{As}$ waveguide structure, one should take a smaller Al concentration x in the UAP (cladding) layer than the Al concentration y in the substrate. One can then find the fill-factor values f_{TE} ; f_{TM} , for which, respectively, $c_{TE} = s$ and $c_{TM} = s$, i.e. the waveguide becomes symmetrical for one of the waves. Figure 4 shows variation of the cut-off thicknesses for a waveguide structure with $x = 0.2$ and $y = 0.7$. In the vicinity of $f = 0.085$ only the TE mode is confined in the interval of $0 < d < d_{c,TE}$ and for $f = 0.145$ only the TM mode is confined in the interval of $0 < d < d_{c,TM}$. Thus, the waveguide with a judiciously chosen fill-factor and active layer thickness can be used as a cutoff-based polarizer. Moreover, region (1') can be extended to higher values of f (which would make the structure easier to make) by using a structure with both core and cladding layers patterned.

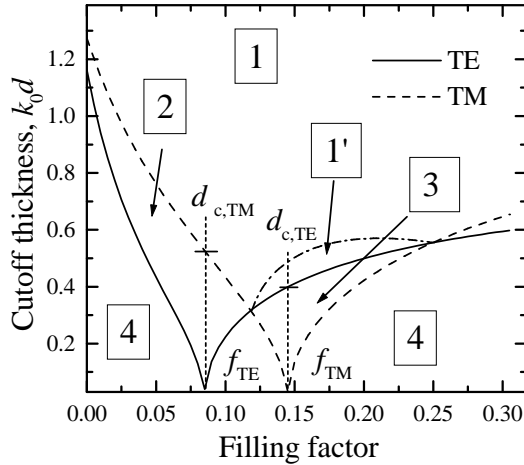


Fig. 4. Cutoff thicknesses for TE and TM modes in an asymmetric structure ($\text{Al}_x\text{Ga}_{1-x}\text{As}/\text{GaAs}/\text{Al}_y\text{Ga}_{1-y}\text{As}$ with $x = 0.2$, $y = 0.7$) as functions of the filling factor of the patterned $\text{Al}_x\text{Ga}_{1-x}\text{As}$ cladding. Vertical lines indicate when the waveguide becomes symmetrical for one of the modes. Regions are designated as in Fig. 3.

C. Dominant lasing mode in highly asymmetric structures

As an example of highly asymmetric waveguide, we consider a structure with air for the cladding layer and a UAP semiconductor core layer (Si , $n_{\text{out}} = 1.2$) on a dielectric substrate (SiN , $n_s = 3.7$). The waveguide profile is illustrated in Fig. 2(b).

First, we calculate the cutoff thicknesses for TE and TM modes. Their dependencies on the fill-factor of the UAP layer are shown in Fig. 5(a). In the range $f = f_c = 0.53$ the TM mode has a smaller cutoff thickness and there is a wide range of thicknesses (region 3) where the waveguide will support only the lowest TM mode. We see that in strongly asymmetric

waveguide structures, at large f , the TM mode has better confinement and larger modal index. This results from the faster growth with f of the asymmetry factor a_{TE} , compared to a_{TM} , see Eqs. (5) and (12). For values of the fill-factor near f_c both modes have a similar confinement factor in a broad range of d , as illustrated in Fig. 5 (b). Note that the values of the confinement factors are generally reduced due to porosity of the core layer.

The examined asymmetric waveguide is similar to that used by Cloutier and Xu [15] who observed a predominantly TM-polarized laser-like emission from a UAP Si-on-insulator layer. The main difference from Fig. 5 is that a lower-index SiO_2 was used as the bottom cladding. It would be tempting to seek an explanation for the observed TM polarization in terms of the UAP properties of the waveguide used. However, the structure parameters in Ref. [15] correspond to $f = 0.18 < f_c$ and for the stated core-layer thickness fall within region 2 of Fig. 5(a). Not only is the TE mode "better" confined, but the TM mode is *not confined at all* at the operating point. Therefore, the observed TM polarization of the generated light in the experiment [15] poses a serious problem, see Appendix II.

D. Polarization switch

Under high illumination the photo-induced concentration of free electrons in the core and/or cladding layer(s) can be large enough for a substantial change of the permittivity and thus effect a change of the modal confinement in a UAP waveguide. Using materials with a short carrier lifetime, both the rise time and the recovery time can be very short, thus providing an ultrafast all-optical modal control. Switching of polarization can be most easily achieved with type-1 structures as in Fig. 2(a), when the optical excitation energy is above the absorption edge of the cladding layer, but below the absorption edge of the substrate layer. In this case, the optical pumping will result in a substantial change of the asymmetry factors for the two modes.

As an example, we consider an asymmetric InGaAsP waveguide [14] operating at $\lambda = 1.55 \mu\text{m}$ with the core layer index $n = 3.55$, the substrate layer index $n_s = 3.24$ and the UAP cladding layer index $n_c = 3.45$. Let the energy of the pump excitation be above the cladding bandgap of $\lambda = 1.35 \mu\text{m}$. The resulting variation of waveguiding can be described by taking the dielectric function of the absorbing core and cladding layers with the Drude contribution of free carriers, viz. $\epsilon = \epsilon_{f1} - \frac{N_i e^2}{m_i (\omega^2 - \omega_{pi}^2)}$ and $\epsilon_{\text{out}} = \epsilon_{c1} - \frac{N_c e^2}{m_c (\omega^2 - \omega_{pc}^2)}$, where $\omega_{pi}^2 = N_i e^2 / m_i$ with ω_{pi} , N_i , and m_i being, respectively, the plasma frequency, the electron-hole pair density, and the reduced effective mass in the core ($i = f$) and the cladding ($i = c$) layers. The bulk optical dielectric constants of the core and cladding materials are denoted, respectively, by ϵ_{f1} and ϵ_{c1} .

Linear decrease of the dielectric function of the core and cladding layers with the free carrier concentration shifts the waveguiding properties and the confinement factors for the two modes. The variation of the cutoff thicknesses is shown in Fig. 6 (case 1). The TM and TE lines intersect at $k_0 d = 0.33$. This means that if we choose the core thickness d to be precisely

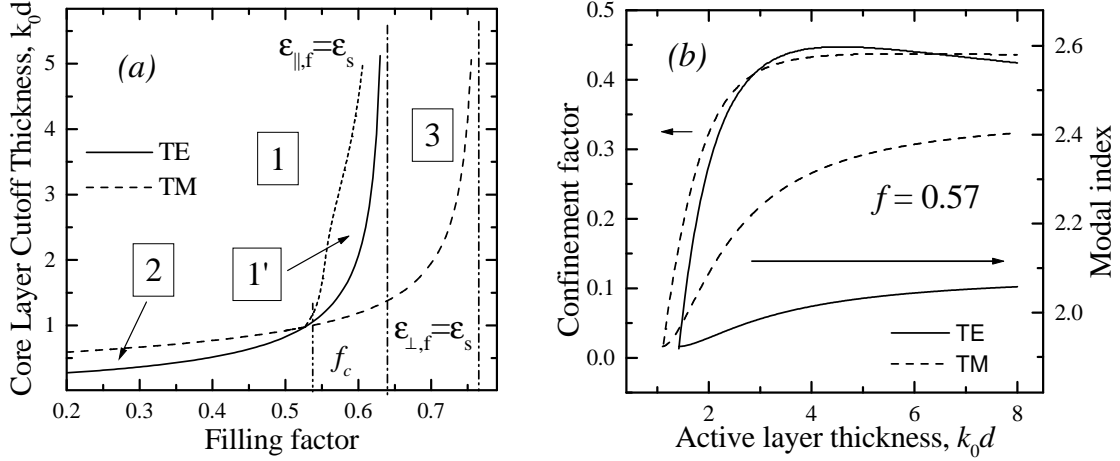


Fig. 5. Cutoff thicknesses and confinement regions for TE and TM modes as a function of fill-factor of the UAP core layer for asymmetric Si/SiN waveguide with air as a cladding layer (a), the regions being noted as in Fig. 3(a); modal indexes and confinement factors for TE and TM modes as a function of core layer thickness for a structure with $f=0.45$ (b).

$\alpha=0.33=k_0$, we shall have only one mode confined for any pumping level. At the pumping corresponding to $N = N_{c,1} = 8.5 \cdot 10^{18} \text{ cm}^{-3}$ the device mode will switch from TM to TE. This effect can be used for both polarization switching and modulation.

The switching concentration $N_{c,1}$ is sensitive to the layer indices and can be adjusted to lower values. For the purpose of low-power switching, more favorable structure is type-3, with both cladding and core layers patterned as in Fig. 2(c). The cutoff thicknesses for this case are also displayed in Fig 6 (case 2). Making both the core and the cladding a UAP layer makes the structure more anisotropic and the free carrier effect on the wave propagation becomes sharper. This lowers the switching concentration $N_{c,2}$.

It is worth noting that if one patterns only the core layer [index profile as in Fig. 2(b)], the photoinduced free carrier concentration would be insufficient to effect a cutoff-controlled switch between the TE and TM modes. The variation of the asymmetry factors is simply not strong enough in this case.

IV. MODAL CONTROL IN LEAKY WAVEGUIDES AND DIRECTIONAL COUPLERS

New useful polarization-dependent effects can be obtained when an additional high-refractive-index layer is added onto the cladding layer, or when the three-layer waveguide is placed on a base-substrate layer of high refractive index. These effects have been exploited in the so-called resonant-layer devices [23], vertical directional couplers and filters [24] and leaky waveguides [25]. Uniaxial patterning of one or more waveguide layers can provide a useful addition to the modal control possibilities of these devices. Here we briefly outline these possibilities.

For waveguides on a high-index base substrate, the main effect of the base substrate results from the exponential decay of the guided modes due to their leakage through the bottom cladding layer into the substrate. (To avoid confusion with the already used term "substrate" for a part of the original

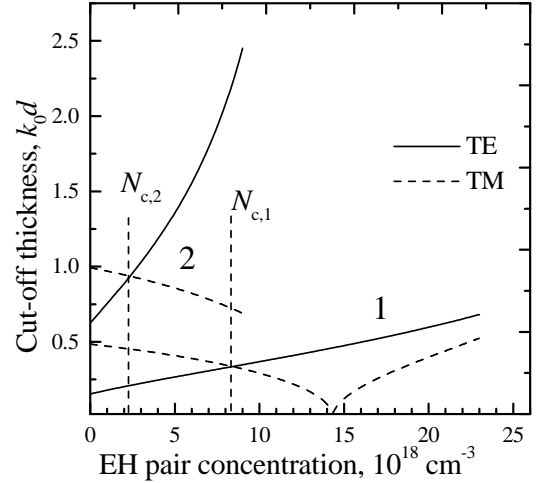


Fig. 6. Cutoff thicknesses for TE and TM modes in an InGaAsP 1.55 μm waveguide structure as functions of the concentration of optically pumped electron-hole pairs. Case (1): UAP cladding layer only; Case (2): both the cladding and the core layers patterned.

waveguide, we are now referring to that layer as "bottom-cladding".) This leakage has an exponentially strong dependence on the difference between the modal effective index and the index of the bottom-cladding layer, which determines the barrier height for photon tunneling decay into the base substrate. In a standard leaky waveguide the TE mode has a higher index and therefore exponentially lower damping. As follows from our discussion in the previous sections, incorporating a UAP layer in the structure allows us to alter the bottom-cladding layer modal transparency. This gives a variable selectivity of the leakage-based modal control.

Adding a high-index resonant layer on the top-cladding layer with its thickness chosen to support a mode with the same propagation constant as the basic waveguide, leads to a well-known oscillatory energy exchange between the two waveguides. The resonant coupling effect underlying this exchange is exponentially sensitive to the matching of the

propagation constants. Incorporation of a UAP layer as a core or a cladding layer, combined with the optical pumping, enables a variable-mode vertical directional coupler that effects fast mode selection at the time of operation.

V. LATERAL VARIATION OF UAP LAYER PARAMETERS

Consider the effect of gradual variation in the density of pores in a UAP cladding layer (vary f laterally). In our limit of $a \gg \lambda$ (even relaxed to $a > \lambda$) the effect is evidently similar to that of lateral index variation in the cladding. It can be used for shaping the mode field in the laser stripe, to achieve desirable properties, similar to those obtained by the parabolic etching of the stripe or the parabolic variation of the material index. An example of such properties is the one-mode high-power generation in a shaped unstable resonator laser design [26], [27]. It is known that one way of obtaining a large gain difference between the fundamental mode and higher-order modes is to use structure profiles with a strong real-index antiguiding and weak imaginary-index guiding. Structures with UAP layers can provide a very effective index antiguiding. In waveguides with a UAP core one must design the pore density so that it is highest at the center line. On the other hand, in waveguides with a UAP cladding layer, the antiguiding effect is achieved when the density of pores (and hence the index contrast) grows with the distance from the center.

We remark that while UAP layers with lateral variation f offer an effective tool for achieving high-power single-mode operation, this approach is rather suitable only for longer wavelength, e.g., for far-infrared devices. One needs room for smooth but sizable pore density variation while still staying in the limit $a > \lambda$.

CONCLUSIONS

We have derived an efficient approach to calculate the cutoff thicknesses and optical confinement factors for a 3-layer semiconductor optical amplifier waveguides with anisotropically patterned layers, in which uniaxial anisotropy is deliberately introduced in one or more of the waveguide layers.

We demonstrate that the patterned layer anisotropy can be efficiently controlled to provide a modal control of various useful waveguide devices. Although no attempt was made to fully optimize the proposed devices, we show that their implementation is within a reasonable range of lithographic and material parameters.

Finally, we note that the theoretical approach used in this work, based on the effective media approximation in the spirit of the Maxwell Garnett theory, has a wider range of validity than that we have exploited so far. Thus, our approach of Sect. V can be used to treat 2-d photonic crystals with laterally varying parameters. The scale of lateral variation does not have to be smooth, so long as the spatial scale of the obtained field variation in the structure exceeds the structure pitch. For example, the same approach can be applied to a 2-d PC with an omitted row of pores that could be useful in the implementation of optical routers and splitters.

APPENDIX I

GUIDING EFFECTS IN A THIN WAVEGUIDE WITH ACTIVE (AMPLIFYING OR ABSORBING) LAYERS

Wave propagation in a 3-layer waveguide with active layers has special features: the waves are inhomogeneous in all layers and hence the wave propagation direction is not the same as the local energy propagation direction. The waveguiding is described by a system of equations, the guiding and the gain/damping effects being interconnected.

We discuss these effects for the case of the TE mode, where we can use the eigenvalue equation (3) for the propagation wave vector in an isotropic layered structure. The TM mode can be considered similarly.

Consider the case of active layers, when $\epsilon_f = \epsilon_f^0 + i\epsilon_f^\infty$. Equation (3) and the equations for $k_{o,f}$; c , and s now have both a real and an imaginary part and split into pairs, e.g.:

$$\begin{aligned} k_{o,f}^0 &= \text{Re} \frac{q}{(\epsilon_f^0 + i\epsilon_f^\infty)k_0^2} \frac{(Q^0 + iQ^\infty)^2}{(Q^0 + iQ^\infty)^2}; \\ k_{o,f}^\infty &= \text{Im} \frac{q}{(\epsilon_f^0 + i\epsilon_f^\infty)k_0^2} \frac{(Q^0 + iQ^\infty)^2}{(Q^0 + iQ^\infty)^2} \end{aligned} \quad (17)$$

The sign of the imaginary parts of the waves should be taken in the usual manner, so that the waves go only out of the layers with larger gain (or into the layers with larger absorption).

Thus, there are two independent variables Q^0, Q^∞ (the complex propagation constant of the wave) and a system of two equations generated by Eq. (3) to find them. The important point is that *all* waves become inhomogeneous if at least one layer is active, $\epsilon_f^\infty \neq 0$, $i = s, c, f$ (excluding the case $\epsilon_s^\infty = \epsilon_f^\infty = 0$).

All qualitative features of the waveguiding can be understood in an exemplary case of a thin core layer, $k_{o,f}d \ll 1$, when Eq. (3) becomes algebraic, viz.

$$k_{o,f}^2 d = c + s \quad (18)$$

Let $Q^2 = k_0^2 z$, $z = x + iy$. Then Eq. (18) reads

$$k_0 d (\epsilon_f^0 + i\epsilon_f^\infty x + iy) = \frac{P}{x + iy} \frac{P}{c} + \frac{P}{x + iy} \frac{P}{s} \quad (19)$$

Let us first discuss the simplest case of a symmetric waveguide, with $c = s$. For this case, equation (19) can be solved by introducing a dimensionless variable, $t = \frac{c}{k_0 d} = \frac{P}{z} \frac{P}{c}$, for which we have

$$k_0 d [\epsilon_f^0 + i\epsilon_f^\infty t^2 - 2it^\infty + t^\infty] = 2(t^0 + it^\infty) \quad (20)$$

where $t^0 = \epsilon_f^0 / c$. Then, we have

$$t^0 + t^\infty k_0 d = 2 = k_0 d (\epsilon_f^0 + t^\infty) = 2; \quad t^\infty = \frac{k_0 d \epsilon_f^\infty}{2(1 + t^0 k_0 d)} \quad (21)$$

Several important conclusions follow from Eq. (21):

First, $t^\infty / \epsilon_f^\infty$. Imaginary part of t is, essentially, the oscillatory contribution to the exponential decay of the wave outside of the core. So, as is physically obvious, it is proportional to ϵ_f^∞ , that is to the difference between the net gain (or loss) in the core and the cladding. This conclusion is not peculiar to the thin layer approximation. It can be anticipated already from the initial equation, but only for a symmetric waveguide. For an asymmetric waveguide, the gain-loss balance is more complicated, see below.

Second, the guiding properties of a thin-core waveguide (they depend only on the sign and the value of τ^0) are determined by two parameters $k_0 d^0$ and $k_0 d^\infty$, of which the former defines the usual "effective one-dimensional potential well" and the latter describes the gain (or loss) guiding effects.

Third, we note that the guiding effects of gain or loss are proportional to the square of the gain differences in the core and the cladding, so that layers with step-like absorption are equally good for guiding. However, for a thin core with gain but no index step, the guiding [described by $\text{Re}(\tau)$] is weak, being proportional to third power of the small parameter $k_0 d$.

Fourth, we note that even in the case of pure gain variation (i.e. $\tau^0 = 0$), the effect is true guiding. Indeed, the core loses its energy only to support the growth of the wave in the adjacent cladding layer. Inasmuch as the wave amplitude and its energy both decrease exponentially away from the core, the guiding can be characterized as confinement (hence we retain the possibility to evaluate energy out of the waveguide). Interestingly, the same is true for a lossy core, when the profile of the wave is essentially maintained by extracting the energy from adjacent layers.

Finally, for our case of a thin core, the equations can be readily solved perturbatively, that is by keeping in first approximation only the lowest terms in $k_0 d$. For τ_c this yields

$$\tau_c^0 = k_0^2 d^0 = 2; \quad \tau_c^\infty = k_0^2 d^\infty = 2 \quad (22)$$

Therefore, in this approximation there is no gain guiding, but it appears when higher terms in $k_0 d$ are taken into account. To bring the discussion in closer correspondence to the results of section II-A, we note that τ is identical to the τ_{TE} , see Eq. (7). We can use Eq. (7) to write down the modal index directly:

$$n_{eff, TE} = \frac{P}{c + \tau^2} = \frac{P}{c^0 + \frac{2}{\tau_{TE}^2} + i[\frac{\tau_c^\infty}{c^0} + \frac{(k_0 d)^2}{2} \frac{\tau_c^0}{c^0}]} \quad (23)$$

In connection with Eq. (23) we make two observations: (i) the second term in the numerator of Eq. (23) gives the well-known Dumke result [20] for the confinement factor (the energy confinement has an additional factor of 2); and (ii) in a waveguide with a thin core and weak confinement, the damping in the cladding is more effective than the gain in the core.

For a symmetric waveguide of arbitrary core thickness, the gain-guiding effects were recently considered by Siegman [28]. Our analytical treatment is restricted to the thin-core limit but it allows to consider the asymmetric waveguide in a similar fashion.

For the asymmetric case we retain the definition of the cutoff as the thickness that borders the region where the real part $\text{Re}(\tau)$ of Eq. (18) vanishes. For a thin core this cutoff thickness can be found directly from the Eq. (7), having in mind that at the cutoff $\text{Re}(\tau_{TE}) = 0$. Damping or gain effects shift the cutoff thickness. This results from the quadratic in τ_c^∞ antiguiding contribution to τ_{TE} .

An important additional issue in an asymmetric waveguide results from the different sign of the propagative contribution to the $\text{Im}(\tau)$ from the asymmetry factor. Indeed, from Eq. (25)

we have

$$\tau = k_0 d (\epsilon_f - \epsilon_s) \frac{P}{\epsilon_s - \epsilon_c} \quad (24)$$

For $k_0 d \ll 1$ we have $\tau^2 \approx \epsilon_f - \epsilon_s$ so that to the lowest order in $k_0 d$ instead of Eq. (7) above equation (24) gives

$$\tau_c = k_0 d (\epsilon_f - \epsilon_s) \frac{P}{\epsilon_s - \epsilon_c} \quad (25)$$

Two remarks are in order here. Firstly, we observe that Eq. (25) coincides with the reduced Eq. (7). Indeed, for τ to be $\ll 1$ the numerator in Eq. (7) should be much smaller than the denominator, so that one can regard the numerator as the difference of two squared and nearly equal terms. Secondly, we note that we obtain the cutoff thickness for a thin layer with low confinement by setting $\text{Re}(\tau) = 0$ in Eq. (25).

Separating imaginary part of Eq. (25) we obtain

$$\text{Im}(\tau_{TE}) = k_0 d \text{Im}(\epsilon_f - \epsilon_s) \frac{P}{\epsilon_s - \epsilon_c} \quad (26)$$

For a confined mode the second term in Eq. (26) is smaller than the first term, but it depends on the difference $(\epsilon_s - \epsilon_c)$ and shows the redistribution of loss between the substrate and the cladding. For a weak confinement, the penetration depth into the substrate is larger than that into the cladding, so that the substrate contribution prevails. As we decrease d , the first term becomes eventually smaller than the second and the confinement is lost.

APPENDIX II EXPERIMENT OF CLOUTIER AND XU [15]

These authors employed a thin 65-nm UAP Si core layer with a fill-factor of $f = 0.18$, a thick SiO_2 bottom cladding on a Si substrate, and air for the top cladding. Under optical pumping they observed light emission at $\lambda = 1278$ nm with many characteristics of laser radiation, unpolarized below threshold and predominantly TM-polarized above the threshold.

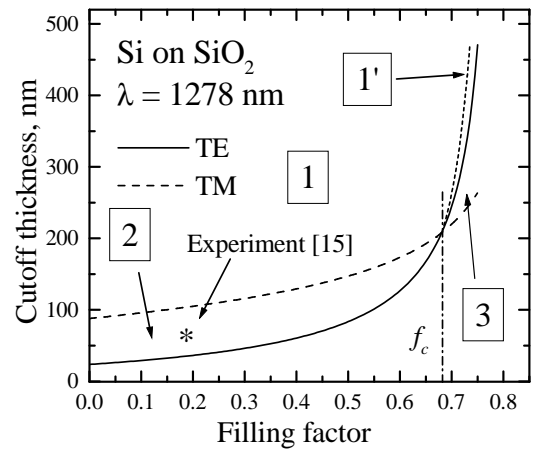


Fig. 7. Cutoff thicknesses for TE and TM modes for a patterned 65 nm-thick Si layer on SiO_2 substrate layer as a function of filling factor. Regions of mode confinement are denoted as in Fig. 3.

The cutoff thicknesses for the two modes at this wavelength are displayed in Fig. 7. We see that except at very high filling factors the TE mode is better confined. That by itself

could be, in principle, overwhelmed by other factors. For example, one could have a peculiar radiative mechanism that favors p polarization. This, however, would also lead to TM polarization below threshold, contrary to observations [15]. A more reasonable explanation, therefore, would be associated with mode-selective feedback mechanism, e.g. higher mirror reflectivity for the TM mode.

However, the problem in interpreting the experiment [15] is not that the TM mode loses the competition with TE, but the fact that at the reported parameters of the structure, the TM mode is not confined at all. The reason for this lack of confinement is the strong asymmetry of the air-clad waveguide.

In principle again, the absence of confinement in a passive waveguide does not preclude the possibility that the TM mode may still be supported by an active finite-length waveguide with gain and feedback. In order for this to happen, the material gain should substantially exceed the rate of leakage [in cm^{-1}] of the unconfined mode into the substrate. For the TM mode this leakage rate at the parameters of the experiment is very high (estimated to be about 10^4 cm^{-1}) and the required gain appears quite unrealistic.

The situation would be rather different if the waveguide were made more symmetric by adding a top cladding layer of refractive index similar to that of the SiO_2 bottom cladding layer. In this case the value of ϵ_c would become much smaller and the cutoff thickness for the TM mode would be strongly reduced. This could be enough to shift the structure parameters to regions 1⁰ or even 3, where the TM mode is dominant.

REFERENCES

- [1] E. Yablonovitch, "Inhibited Spontaneous Emission in Solid-State Physics and Electronics," *Phys. Rev. Lett.*, vol. 58, no. 20, pp. 2059-2062, 1987.
- [2] O. Painter, R. K. Lee, A. Scherer, A. Yariv, J. D. O'Brien, P. D. Dapkus, and I. Kim, "Two-dimensional photonic band-gap defect mode laser," *Science* vol. 284, no. 5421, pp. 1819-1821, 1999.
- [3] S. G. Johnson, Sh. Fan, P. R. Villeneuve, J. D. Joannopoulos, and L. A. Kolodziejski, "Guided modes in photonic crystal slabs," *Phys. Rev. B*, vol. 60, no. 8, 5751-5758, 1999.
- [4] M. Plihal, and A. A. Maradudin, "Photonic band structure of two-dimensional systems: The triangular lattice," *Phys. Rev. B*, vol. 44, no. 16, pp. 8565-8571, 1991.
- [5] J. D. Joannopoulos, R. D. Meade, and J. N. Winn, *Photonic Crystals: Molding the Flow of Light* (Princeton University, Princeton, NJ, 1995).
- [6] J. C. Maxwell Garnett, "Colours in Metal Glasses and in Metallic Films," *Philosophical Transactions of the Royal Society of London. Series A*, vol. 203, pp. 385-420, 1904.
- [7] N. A. Nicorovici, R. C. McPhedran, and L. C. Botten, "Photonic band gaps: noncommuting limits and the 'acoustic band'," *Phys. Rev. Letters*, vol. 75, no. 8, pp. 1507-1520, 1995.
- [8] A. K. Sarychev, and V. M. Shalaev, "Electromagnetic field fluctuations and optical nonlinearities in metal-dielectric composites," *Physics Reports*, vol. 335, no. 6, pp. 275-371, 2000.
- [9] F. Genereux, S. W. Leonard, and H. M. van Driel, "Large birefringence in two-dimensional silicon photonic crystals," *Phys. Rev. B* 63, no. 16, pp. 161101-161105, 2001.
- [10] P. Halevi, and F. Ramos-Mendieta, "Tunable Photonic Crystals with Semiconducting Constituents," *Phys. Rev. Lett.*, vol. 85, pp. 1875-1878, 2000.
- [11] A. A. Krokhin, P. Halevi, and J. Arriaga, "Long-wavelength limit (homogenization) for two-dimensional photonic crystals," *Physical Review B*, vol. 65, no. 11, pp. 115208, 2002.
- [12] M. J. Adams, *An Introduction to Optical Waveguides* (Wiley, New York, 1981).
- [13] T. D. Visser, H. Blok, B. Demeulenaere, and D. Lenstra, "Confinement factors and gain in optical amplifiers," *IEEE J. Quant. Electron.*, vol. 33, no. 10, pp. 1763-766, 1997.
- [14] Y-Z. Huang, Z. Pan, and R-H. Wu, "Analysis of optical confinement in semiconductor lasers," *J. Appl. Phys.*, vol. 79, no. 8, pp. 3827-3830, 1996.
- [15] C. Cloutier, and J. Xu, "Laser-like emission from a periodic all-silicon nanostructure", arxiv: cond-mat/0412376, 2004.
- [16] X. Wu, A. Yamilov, X. Liu, S. Li, V. P. Dravid, R. P. H. Chang, and H. Cao, "Ultraviolet photonic crystal laser", arxiv: physics/0406005, 2004.
- [17] M.D.B. Charton, S.W. Roberts, and G. J. Parker, "Guided mode analysis and fabrication of a 2-dimensional visible photonic band structure confined within a planar semiconductor waveguide," *Materials Science and Engineering B*, vol. 48, pp. 155-165, 1998.
- [18] We note that in the case considered ($n_{in} < n_{out}$) the "average" index $\langle n \rangle$ is rather close to n_{in} . However, in the opposite case of $n_{in} > n_{out}$ (dielectric cylinders in air), the value of $\langle n \rangle$ is intermediate between the true refractive indices for the two polarizations and differs strongly from both.
- [19] In addition, the difference in the reflection coefficients for the two modes also favors the TE mode generation. It is however, less important for a long enough cavity and can be easily taken into account.
- [20] H. C. Casey and M. B. Panish, *Heterostructure Lasers; Part A: Fundamental Principles*. New York: Academic, 1978, pp. 54-57.
- [21] J. Buus, "Analytical approximation for the reflectivity of DH lasers," *IEEE Journal of Quantum Electronics*, vol. 17, no. 12, pp. 2256-2257, 1981.
- [22] M. Levinshtein, S. Rumyantsev, and M. Shur, *Handbook Series on Semiconductor Parameters*, vol. 1., World Scientific, London, 1999.
- [23] J.M. Hammer, G.A. Evans, G. Ozgur, and J. K. Butler, "Isolators, Polarizers, and Other Optical Waveguide Devices Using a Resonant-Layer Effect," *J. of Lightwave Technology*, vol. 22, no. 7, pp. 1754-1763, 2004.
- [24] K.J. Ebeling, *Integrated Opto-electronics*, Springer-Verlag, Berlin 1993, pp.143-170.
- [25] L. Torner, F. Canal, and J. Hernandez-Marco, "Leaky modes in multi-layer uniaxial optical waveguides", *Applied Optics*, vol. 29, no. 18, pp. 2805-2814, 1990.
- [26] S. Guel-Sandoval, A. H. Paxton, S. T. Srinivasan, Sh.Sun, S. D. Hersee, M. S. Allen, Ch. E. Moeller, D. J. Gallant, G. C. Dente, and J. G. McInerney, "Novel high-power and coherent semiconductor laser with a shaped unstable resonator", *Applied Physics Letters*, vol. 66, no. 16, pp. 2048-2050, 1995.
- [27] A. K. Chan, C. P. Lai, and H. F. Taylor, "Antiguinding index profiles in broad strip semiconductor lasers for high-power, single-mode operation", *IEEE Journal of Quantum Electronics*, vol. 24, no. 3, pp. 489-495, 1988.
- [28] A. E. Siegman, "Propagating modes in gain-guided optical fibers", *Journal of the Optical Society of America A*, vol. 20, no. 8, pp. 1617-1628, 2003.